DOI: 10.1002/anie.200701348

Computational Biology

Deprotonation Mechanism of NH_4^+ in the *Escherichia coli* Ammonium Transporter AmtB: Insight from QM and QM/MM Calculations**

Zexing Cao, Yirong Mo,* and Walter Thiel*

Ammonia is the primary nitrogen source for the biological synthesis of amino acids in microorganisms and plants.[1,2] In animals and humans, renal and hepatic ammonia sequestration and excretion are of fundamental importance for the regulation of the systemic pH value and the functioning of the central nervous system.[3] The weak base ammonia exists predominantly (> 99 %) in the form of the NH_4^+ cation under physiological conditions. The uptake and secretion of ammonia is mediated by membrane proteins, including the ammonia transporter (Amt),[4] methylammonium/ammonium permease (Mep),[2,5] and the Rhesus (Rh) protein.[6] The transport rate has been measured to be 10^1–10^4 ammonia molecules per second per transporter.[7]

Recently, the X-ray crystal structure of the ammonia-channel protein AmtB from *Escherichia coli* was determined at a resolution of 1.35 Å.[8] The structure reveals a 20-Å-long hydrophobic channel and an extracellular recruitment (binding) vestibule for NH_4^+ just outside of the channel. The vestibule comprises the residues Phe103, Phe107, Trp148, and Ser219. It had been assumed that the π–cation interactions between the aromatic rings in the binding vestibule and NH_4^+ stabilize the latter, but recent theoretical work has identified a strong electrostatic interaction between the externally bound NH_4^+ cation and the carboxy group of Asp160, which are separated by approximately 8 Å, as the principal stabilizing force.[9] Similar structural characteristics were observed in the structure of Amt-1 from *Archaeoglobus fulgidus*.[10] The most significant finding from the experimental crystal structures of Amt proteins is that ammonia molecules (NH_3) rather than ammonium ions (NH_4^+) are the transported species, as deduced from the high hydrophobicity of the channels. Molecular-dynamics (MD) simulations on the mechanisms of substrate binding and NH_3/NH_4^+ transport in AmtB confirmed this view.[9,11,12] Thus, NH_4^+ must lose a proton before it passes through the channel, and the elucidation of the deprotonation mechanism is critical for the understanding of the function and structure of ammonia-transport proteins. MD simulations with molecular-mechanical (MM) potentials suggest that Asp160, which is highly conserved in ammonia-transport proteins and whose replacement with other residues reduces or disables transport ability,[13,14] is probably the transient proton acceptor.[11] As the proton transfer, which is mediated by water, involves the breaking and formation of several chemical bonds, an accurate description of the process requires high-level quantum-mechanical (QM) treatment. Herein, we describe the detailed exploration of the deprotonation process with density functional theory (DFT) and combined QM/MM methods.

The complete computational model was constructed by solvating the crystal structure of AmtB (PDB code: 1U7G)[8] in a sphere of water molecules with a radius of 30 Å and then carrying out MM–MD simulations with CHARMM[15] for 30 ps to bring the system to an equilibrium state. This model contains 13155 atoms and includes the AmtB protein and 2483 water molecules. The equilibrated configuration (Figure 1) was used as the starting point for the subsequent pure QM and combined QM/MM calculations. The QM calculations (approach 1) involved only the reactive site, which consists of NH_4^+ and all residues around the cation within a distance of 5 Å; the resulting QM cluster model for pure DFT treatment contains 180 atoms. The BLYP functional[16] and the basis set "double numerical plus d functions" (DND), as well as the DND basis set augmented by polarization functions (DNP) as implemented in the DMol3 package,[17] were employed in the DFT calculations. The QM/MM calculations (approach 2) involved a QM region with 149 QM atoms (in selected residues around NH_4^+ and within 5 Å of the cation) and 13106 MM atoms. In the QM/MM geometry optimizations, the QM region and 1774 MM atoms (defined by including all atoms around NH_4^+ within a distance of 13 Å) were allowed to relax, whereas the remaining MM atoms were constrained. The QM part was treated at the B3LYP/6-31G(d) level, and the MM part was described by the CHARMM22 force field.[18] An electronic embedding scheme[19] was adopted, and the ChemShell

[*] Prof. Dr. Z. Cao
Department of Chemistry and
State Key Laboratory of Physical Chemistry of Solid Surfaces
Xiamen University
Xiamen 361005 (China)
Fax: (+86) 592-218-4708
E-mail: zxcao@xmu.edu.cn
Prof. Dr. Y. Mo
Department of Chemistry
Western Michigan University
Kalamazoo, MI 49008 (USA)
Fax: (+1) 269-387-2909
E-mail: yirong.mo@wmich.edu
Prof. Dr. W. Thiel
Max-Planck-Institut für Kohlenforschung
Kaiser-Wilhelm-Platz 1, 45470 Mülheim an der Ruhr (Germany)

[**] This research was supported financially by the National Science Foundation of China (20673087, 20473062, 20423002) and the Ministry of Science and Technology of China (2004CB719902). Z.C. acknowledges the financial support of the Alexander von Humboldt Foundation during his stay at the Max-Planck-Institut für Kohlenforschung. We thank Dr. D. Wang and Dr. H. Lin for helpful discussions.

Supporting information for this article (details of semiclassical KIE estimates and data for thermodynamic integration) is available on the WWW under http://www.angewandte.org or from the author.

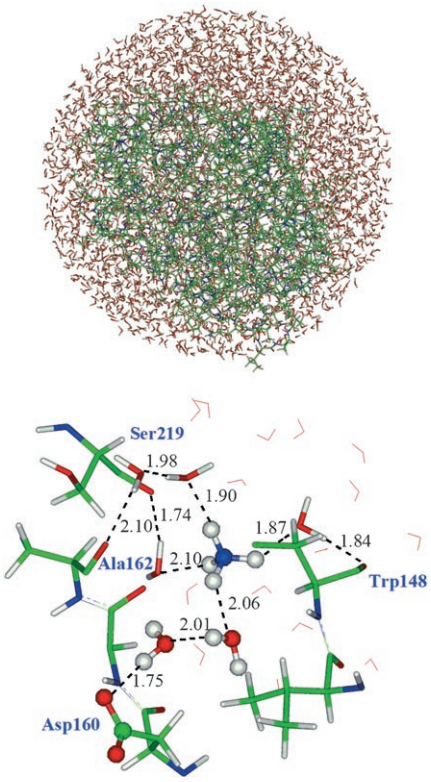

Figure 1. Equilibrated configuration used as the starting point for subsequent QM and QM/MM geometry optimization.

package,[20] in which the Turbomole[21] and DL-POLY[22] programs were integrated, was employed to carry out the QM/MM calculations.

In the QM/MM MD simulations (approach 3), the QM region was reduced to either 15 QM atoms (model **3A**) or 51 QM atoms (model **3B**; Figure 2), and the 6-31G(d) and 6-31G basis sets were employed for models **3A** and **3B**, respectively. As quite a complicated H-bond network is present in these structures, all QM/MM MD simulations were performed at the BLYP/CHARMM level with the ChemShell package,[20] which provided the QM/MM coupling engine and the MD driver. The active MM region in the QM/MM MD simulations was composed of all residues around NH_4^+ within 10 Å of the cation. The optimal structure of **Asp-NH_4^+** (Figure 3) from approach 2 was taken as the initial state for configuration sampling. The reaction coordinate (RC) was defined as RC = R1−R2 (see Figure 2). The QM/MM MD setup and thermodynamic-integration approach were introduced in a previous study.[23] The subsequent simulations were performed at T = 300 K under the conditions of a NVT canonical ensemble (that is, each system in the ensemble has the same number of particles and the same volume, and the temperature is well defined). The system was first heated by a Berendsen thermostat for 1 ps, then equilibrated by the Nose–Hoover thermostat for another 1 ps. It was then sampled every 0.5 ps along the reaction coordinate, and the restart files for all points (windows) on the reaction coordinate were prepared. Finally, each point on the reaction coordinate was equilibrated for 0.5 ps to collect the data for thermodynamic integration. Statistical tests, such as the Mann–Kendall test for trend, the Shapiro–Wilk W test for normality, and the von Neumann test for serial correlation, were performed to establish converged averages.

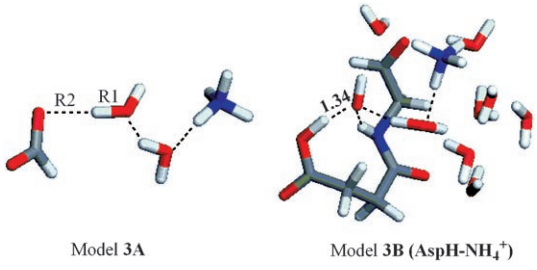

Figure 2. QM models used in the QM/MM MD simulations. Model **3B** is the equilibrated configuration of **AspH-NH_4^+**.

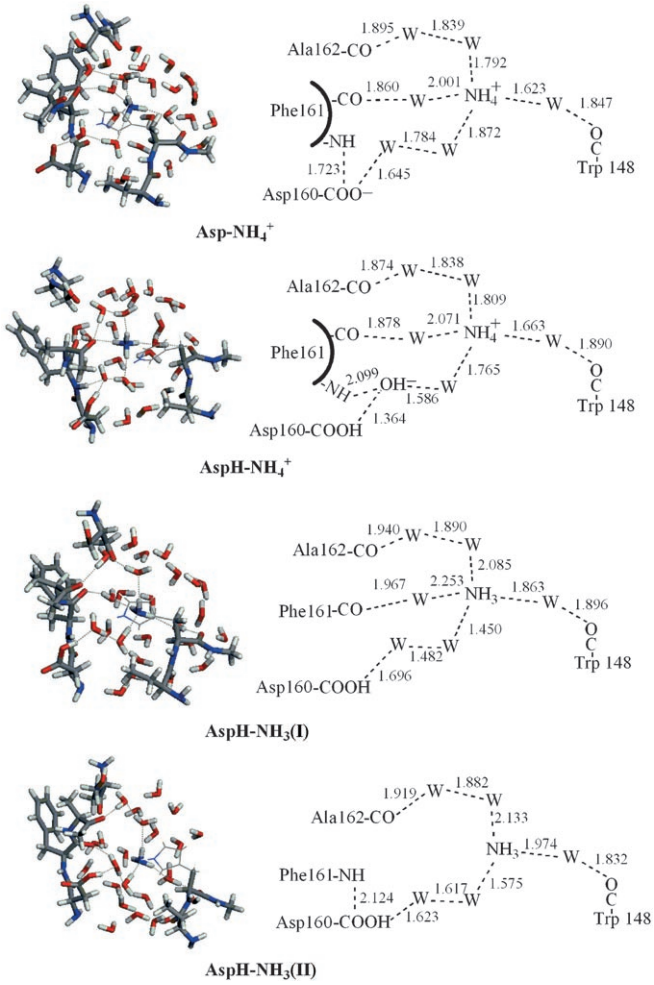

Figure 3. Optimal conformations involved in proton transfer from NH_4^+ to the carboxylate group of Asp160 by approach 1 at the BLYP/DND level.

The MD simulations, as well as the QM and QM/MM calculations, revealed that NH_4^+ is stabilized in the binding vestibule of AmtB by a hydrogen-bond network around the cation. In particular, there is a hydrogen-bond wire mediated

by two water molecules between NH_4^+ and the carboxylate group (CO_2^-) of Asp160 (Figures 3 and 4). This finding is in agreement with the results of previous MD simulations,[11] and similar proton-transfer pathways exist in many biochemical processes, such as water-assisted intramolecular proton transfer between zinc-bound water and His64 in carbonic anhydrase II (CAII).[24] In the current case, the deprotonation of NH_4^+ and transfer of the proton to Asp160 could occur by a concerted hopping of protons between water molecules in a manner analogous to the Grotthuss mechanism, which explains the anomalously high mobility of protons in water,[25] or by a stepwise mechanism in which the proton is first transferred from NH_4^+ to the adjacent water molecule, then to the next water molecule, and finally to the carboxylate group. However, it is also possible that the negative rather than the positive charge migrates. In this case, the carboxylate group first abstracts a proton from the water molecule close to it, and the resulting hydroxide ion abstracts a proton from another water molecule, which in turn abstracts a proton from NH_4^+. This alternative to the Grotthuss mechanism for proton transfer in solution and in CAII was investigated recently by Cui and co-workers.[26] In the study described herein, we probed proton transfer from NH_4^+ to Asp160 through the hydrogen-bond wire by QM (approach 1) and QM/MM optimizations (approach 2), as well as by QM/MM MD simulations (approach 3). The linear-synchronous-transit approach was used to generate a reaction path by geometric interpolation between the reactant and the product. This reaction path served as the starting point for the subsequent transition-state search.

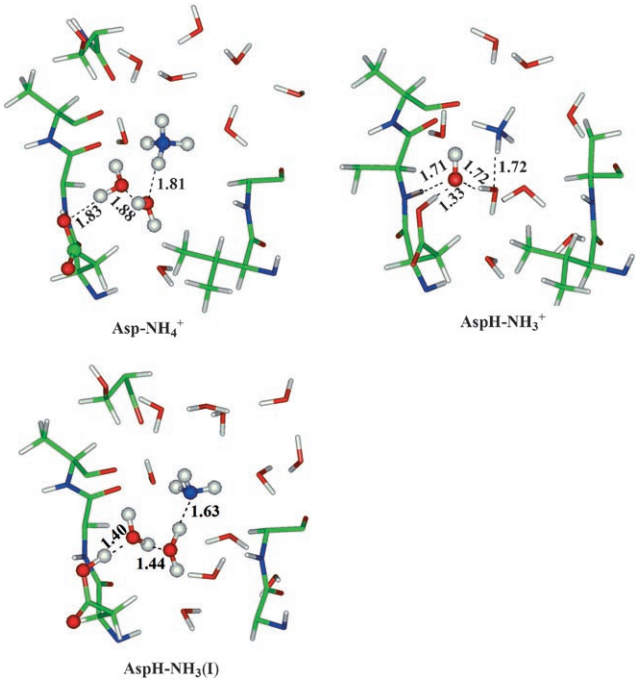

Figure 4. Optimal conformations involved in proton transfer from NH_4^+ to the carboxylate group of Asp160 by approach 2 (QM: B3LYP/6-31G(d), MM: CHARMM).

Figure 5 depicts the predicted relative-energy profile for the proton-transfer process by approach 1 at the BLYP/DND level with zero-point-energy (ZPE) corrections; Table 1 presents for comparison the relative energies (without ZPE corrections) found by various approaches for selected key conformations involved in the proton transfer. All calculations lead to the conclusion that a stepwise mechanism is involved. If we restrict the proton-transfer process to a concerted mechanism, the energy barrier would be as high as approximately 30 kcal mol^{-1}. In the stepwise route, Asp160 in the initial conformation (**Asp-NH_4^+**, Figure 3) accepts one proton to give **AspH-NH_4^+**, which contains a hydroxy anion. The ZPE-corrected energy barrier for this process is 7.2 kcal mol^{-1}. The generation of a hydroxide ion (OH^-) in this step seems very unusual, as the hydrolysis of water molecules normally occurs at a transition-metal-ion center, whereby the subsequent binding of OH^- to the metal ion lowers the energy barrier to reaction significantly and stabilizes the system. In our case, the hydroxide ion is stabilized by three hydrogen bonds, namely, Asp-COOH···OH^-, HOH···OH^-, and Phe161-NH···OH^-, and as a consequence, the **AspH-NH_4^+** conformation is less stable than **Asp-NH_4^+** by only 6.9 kcal mol^{-1}. Previous BLYP-based MD simulations demonstrated that similar conformations of hydrated OH^- ions with threefold coordination of the oxygen atom play a crucial

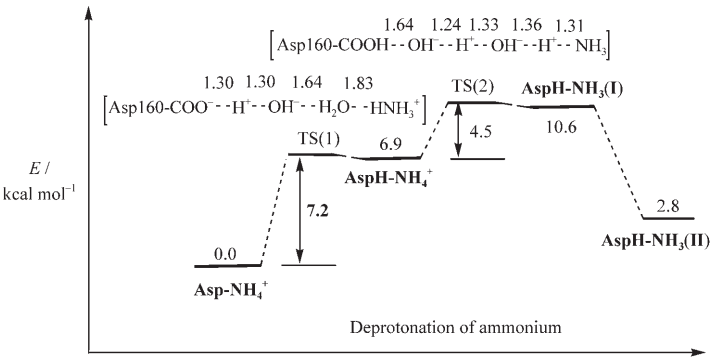

Figure 5. Relative-energy profile with zero-point-energy corrections for the deprotonation of NH_4^+ and transfer of the proton to Asp160 through the mediation of two water molecules. The data are derived from QM calculations at the BLYP/DND level. TS: transition state.

Table 1: Relative energies [kcal mol^{-1}] of species involved in the deprotonation of NH_4^+ in AmtB, as measured by approaches 1 and 2.[a]

Level	Asp-NH_4^+	AspH-NH_4^+	AspH-NH_3(I)	AspH-NH_3(II)
BLYP/DND	0.0	6.6	14.5	4.1
BLYP/DNP	0.0	7.0	14.6	4.2
B3LYP/6-31G(d)	0.0	8.4	18.3	8.8
QM/MM	0.0	5.0 (2.6)	17.5 (14.7)	

[a] The first three levels correspond to QM calculations (approach 1). The QM/MM optimizations (approach 2) were performed with the QM basis set B3LYP/6-31G(d) (or for the results in parentheses, BLYP/6-31G(d)).

role in the fast transport of OH^- ions in aqueous solution.[27] The subsequent concerted proton transfer from NH_4^+ to OH^- via one water molecule yields a metastable species **AspH-NH_3(I)** and has an energy barrier of 4.5 kcal mol^{-1}. With the relaxation of the surrounding hydrogen-bond network, **AspH-NH_3(I)** evolves into the final conformation **AspH-NH_3(II)**, which is stabilized by 7.8 kcal mol^{-1} relative to **AspH-NH_3(I)** but slightly higher in energy (by 2.8 kcal mol^{-1}) than the initial conformation **Asp-NH_4^+**. The overall proton-transfer process has a change in Gibbs free energy, ΔG, of -1.8 kcal mol^{-1} at 298.15 K. We note that other QM and QM/MM calculations result in comparable data, as shown in Table 1, and that the ZPE is significant for **AspH-NH_3(I)**.

The results of the QM and QM/MM calculations showed that the first transition states, for proton transfer to Asp160 and the resulting intermediate **AspH-NH_4^+**, are located at RC values of 0.0 (Figure 5) and 0.24 Å, respectively. We performed further QM/MM MD simulations (approach 3) to derive the free-energy profiles along the reaction coordinate from the initial state to these points (Figure 6). The MD

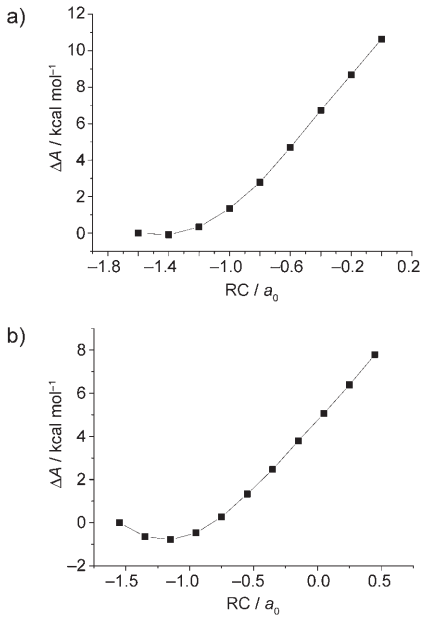

Figure 6. Free-energy profiles along the reaction coordinate as obtained by QM/MM MD simulation. a_0: the atomic units (Bohrs); RC = R1 − R2 (see Figure 2): a) model **3A**; b) model **3B**.

simulations with model **3A** indicated that the change in free energy for the proton transfer at RC = 0.0 is 10.6 kcal mol^{-1} (Figure 6a), whereas simulations with model **3B** predicted that the change in free energy for the generation of the first intermediate (**AspH-NH_4^+** at RC ≈ 0.45 Bohr) by proton transfer is 7.8 kcal mol^{-1} (Figure 6b). As the ZPE corrections were not taken into account in the simulations, we conclude that the results of the QM/MM simulations are consistent with the data in Figure 5 (7.2 and 6.9 kcal mol^{-1}, respectively).

As all approaches in this study suggest that the first step from **Asp-NH_4^+** to **AspH-NH_4^+** is rate limiting for the whole proton-transfer process, we estimated its proton-tunneling effect with the simple Wigner tunneling correction for the QM model of 180 atoms (for details, see the Supporting Information). We first calculated a semiclassical kinetic isotope effect (KIE) of 6.2 and then derived the Wigner tunneling-corrected KIE. As the latter value of 8.1 is larger than the former value, we conclude that there is a quantum-mechanical tunneling effect in AmtB. However, there is quite a low energy barrier to the deprotonation of NH_4^+ (7.2 kcal mol^{-1}), and the tunneling effect may be not significant in this case. Although to date no experimental results on the KIE in AmtB have been reported, the importance of proton tunneling in enzyme-catalyzed reactions is well recognized.[28]

In the proton-transfer process, the hydrogen-bond network between NH_4^+ and the residues Trp148, Ala162, and Asp160 is retained, but remarkable changes are observed for Phe161. In the initial conformation **Asp-NH_4^+**, there is a strong hydrogen-bonding interaction between the carboxy group of Asp160 and the backbone NH group of Phe161. This hydrogen bond is lost after the first proton transfer, as the NH group then points toward the hydroxide ion (OH^-) in **AspH-NH_4^+**. After the final proton transfer, the NH group of Phe161 returns to its initial position in the product conformation **AspH-NH_3(II)**.

In summary, the QM and QM/MM optimizations and QM/MM MD simulations show that the carboxylate group of Asp160 can act as the proton acceptor in the deprotonation of NH_4^+ mediated by two water molecules. The calculations support a stepwise rather than a concerted mechanism. The water molecule close to the carboxy group first loses a proton to form a hydroxide ion, which is stabilized significantly by hydrogen bonding to the protonated carboxylate group of Asp160, the backbone NH group of Phe161, and a water molecule. The tunneling-corrected KIE value for the first proton transfer is 8.1, which suggests a certain tunneling effect in this step. The subsequent proton transfer from NH_4^+ to the hydroxide ion via one water molecule completes the proton-transfer process. The present study rationalizes the role of the preserved residue Asp160 and clarifies why mutations of Asp160 reduce or disable the activity of AmtB.[13]

Received: March 28, 2007
Revised: May 14, 2007
Published online: August 2, 2007

Keywords: ammonia transport · computational biology · density functional calculations · hydrogen bonds · molecular dynamics

[1] O. Ninnemann, J. C. Jauniaux, W. B. Frommer, *EMBO J.* **1994**, *13*, 3464 – 3471; N. von Wirén, S. Gazzarrini, A. Gojon, W. B. Frommer, *Curr. Opin. Plant Biol.* **2000**, *3*, 254 – 261; J. B. Howard, D. C. Rees, *Chem. Rev.* **1996**, *96*, 2965 – 2982.
[2] G. H. Thomas, J. G. Mullins, M. Merrick, *Mol. Microbiol.* **2000**, *37*, 331 – 344.
[3] M. A. Knepper, R. Packer, D. W. Good, *Physiol. Rev.* **1989**, *69*, 179 – 249; N. L. Nakhoul, L. L. Hamm, *Pflugers Arch.* **2004**, *447*, 807 – 812.

[4] A. Jayakumar, S. J. Hwang, J. M. Fabiny, A. C. Chinault, E. M. J. Barnes, *J. Bacteriol.* **1989**, *171*, 996 – 1001.
[5] A. M. Marini, S. Vissers, A. Urrestarazu, B. Andre, *EMBO J.* **1994**, *13*, 3456 – 3463.
[6] C. H. Huang, J. B. Peng, *Proc. Natl. Acad. Sci. USA* **2005**, *102*, 15512 – 15517; C. Le Van Kim, Y. Colin, J. P. Cartron, *Blood Rev.* **2006**, *20*, 93 – 110; C. M. Westhoff, M. Ferreri-Jacobia, D. O. D. Mak, J. K. Foskett, *J. Biol. Chem.* **2002**, *277*, 12499 – 12502.
[7] L. Zheng, D. Kostrewa, S. Berneche, F. K. Winkler, X. D. Li, *Proc. Natl. Acad. Sci. USA* **2004**, *101*, 17090 – 17095.
[8] S. Khademi, J. O'Connell, J. Remis, Y. Robles-Colmenares, L. J. W. Miericke, R. M. Stroud, *Science* **2004**, *305*, 1587 – 1594.
[9] V. B. Luzhkov, M. Almloef, M. Nervall, J. Aaqvist, *Biochemistry* **2006**, *45*, 10807 – 10814.
[10] S. L. A. Andrade, A. Dickmanns, R. Ficner, O. Einsle, *Proc. Natl. Acad. Sci. USA* **2005**, *102*, 14994 – 14999.
[11] Y. Lin, Z. Cao, Y. Mo, *J. Am. Chem. Soc.* **2006**, *128*, 10876 – 10884.
[12] D. L. Bostick, C. L. Brooks III, *PLoS Comput Biol.* **2007**, *3*, 231 – 246; H. Ishikita, E.-W. Knapp, *J. Am. Chem. Soc.* **2007**, *129*, 1210 – 1215; T. P. Nygaard, C. Rovira, G. H. Peters, M. O. Jensen, *Biophys. J.* **2006**, *91*, 4401 – 4412; H. Yang, Y. Xu, W. Zhu, K. Chen, H. Jiang, *Biophys. J.* **2007**, *92*, 877 – 885.
[13] A. Javelle, E. Severi, J. Thornton, M. Merrick, *J. Biol. Chem.* **2004**, *279*, 8530 – 8538.
[14] A. M. Marini, M. Boeckstaens, F. Benjelloun, B. Cherif-Zahar, B. Andre, *Curr. Genet.* **2006**, *49*, 364 – 374.
[15] B. R. Brooks, R. E. Bruccoleri, B. D. Olafson, D. J. States, S. Swaminathan, M. Karplus, *J. Comput. Chem.* **1983**, *4*, 187 – 217.
[16] A. D. Becke, *J. Chem. Phys.* **1988**, *88*, 2547 – 2553; C. T. Lee, W. T. Yang, R. G. Parr, *Phys. Rev. B* **1988**, *37*, 785 – 789.
[17] B. Delley, *J. Chem. Phys.* **1990**, *92*, 508 – 517; B. Delley, *J. Chem. Phys.* **2000**, *113*, 7756 – 7764; B. Delley, *J. Phys. Chem.* **1996**, *100*, 6107 – 6110.
[18] A. D. MacKerell, D. Bashford, M. Bellott, R. L. Dunbrack, J. D. Evanseck, M. J. Field, S. Fischer, J. Gao, H. Guo, S. Ha, D. Joseph-McCarthy, L. Kuchnir, K. Kuczera, F. T. K. Lau, C. Mattos, S. Michnick, T. Ngo, D. T. Nguyen, B. Prodhom, W. E. Reiher, B. Roux, M. Schlenkrich, J. C. Smith, R. Stote, J. Straub, M. Watanabe, J. Wiorkiewicz-Kuczera, D. Yin, M. Karplus, *J. Phys. Chem. B* **1998**, *102*, 3586 – 3616.
[19] D. Bakowies, W. Thiel, *J. Phys. Chem.* **1996**, *100*, 10580 – 10594.
[20] P. Sherwood, A. H. de Vries, M. F. Guest, G. Schreckenbach, C. R. A. Catlow, S. A. French, A. A. Sokol, S. T. Bromley, W. Thiel, A. J. Turner, S. Billeter, F. Terstegen, S. Thiel, J. Kendrick, S. C. Rogers, J. Casci, M. Watson, F. King, E. Karlsen, M. Sjovoll, A. Fahmi, A. Schafer, C. Lennartz, *J. Mol. Struct.* **2003**, *632*, 1 – 28.
[21] R. Ahlrichs, M. Bär, M. Haser, H. Horn, C. Kölmel, *Chem. Phys. Lett.* **1989**, *162*, 165 – 169.
[22] W. Smith, T. R. Forester, *J. Mol. Graphics* **1996**, *14*, 136 – 141.
[23] H. M. Senn, S. Thiel, W. Thiel, *J. Chem. Theory Comput.* **2005**, *1*, 494 – 505, and references therein.
[24] P. H. König, N. Ghosh, M. Hoffmann, M. Elstner, E. Tajkhorshid, T. Frauenheim, Q. Cui, *J. Phys. Chem. A* **2006**, *110*, 548 – 563, and references therein.
[25] C. J. T. de Grotthuss, *Ann. Chim. Phys.* **1806**, *LVIII*, 54.
[26] D. Riccardi, P. Konig, X. Prat-Resina, H. B. Yu, M. Elstner, T. Frauenheim, Q. Cui, *J. Am. Chem. Soc.* **2006**, *128*, 16302 – 16311.
[27] M. E. Tuckerman, A. Chandra, D. Marx, *Acc. Chem. Res.* **2006**, *39*, 151 – 158; M. E. Tuckerman, D. Marx, M. Parrinello, *Nature* **2002**, *417*, 925 – 929.
[28] J. Pu, J. Gao, D. G. Truhlar, *Chem. Rev.* **2006**, *106*, 3140 – 3169; L. Masgrau, A. Roujeinikova, L. O. Johannissen, P. Hothi, P. Basran, K. E. Ranaghan, A. J. Mulholland, M. J. Sutcliffe, N. S. Scrutton, D. Leys, *Science* **2006**, *312*, 237 – 241; S. Hammes-Schiffer, *Acc. Chem. Res.* **2006**, *39*, 93 – 100.

